

Cold Optical Injection Producing Monoenergetic, Multi-GeV Electron Bunches

X. Davoine,^{1,*} E. Lefebvre,¹ C. Rechatin,² J. Faure,² and V. Malka²

¹CEA, DAM, DIF, Bruyères-le-Châtel, 91297 Arpajon, France

²Laboratoire d'Optique Appliquée, ENSTA, CNRS, Ecole Polytechnique, UMR 7639, 91761 Palaiseau, France

(Received 20 November 2008; published 10 February 2009)

A cold optical injection mechanism for a laser-plasma accelerator is described. It relies on a short, circularly polarized, low-energy laser pulse counterpropagating to and colliding with a circularly polarized main pulse in a low density plasma. Contrary to previously published optical injection schemes, injection is not caused here by electron heating. Instead, the collision between the pulses creates a spatially periodic and time-independent beat force. This force can block the longitudinal electron motion, leading to their entry and injection into the propagating wake. In a specific setup, we compute after acceleration over 0.6 mm, a 60 MeV, 50 pC electron bunch with 0.7 MeV rms energy spread, proving the interest of this scheme to inject electron bunches with a narrow absolute energy spread. Acceleration to 3 GeV with a rms spread smaller than 1% is computed after propagation over 3.8 cm in a plasma channel.

DOI: 10.1103/PhysRevLett.102.065001

PACS numbers: 52.38.Kd

Over the past few years, striking progress on laser-wakefield acceleration of electrons [1] has been achieved. In particular, since the production of the first experimental quasimonoenergetic spectra [2–4], GeV energy has been reached [5,6], guided propagation [7] and acceleration [5] in a capillary have been demonstrated, and the use of optical injection has proven that stabilization and control of electron beams are possible [8]. Further developments of laser-wakefield accelerators reside in the improvement of the beam energy and quality, overall system stability, and reproducibility. In this Letter, we report on a new scheme for optical injection that enables injection of narrow-energy-spread bunches in low-plasma-density wakefields, allowing large energy gain. Control of injection with an all-optical method, high energy gain, and narrow energy spread are thus the major interests of the proposed method.

Optical injection was first proposed in Ref. [9]. In this scheme, injection is triggered by a second laser pulse (injection pulse) coming perpendicularly to the pulse generating the wakefield (pump pulse). When the injection pulse collides with the wakefield, the transverse ponderomotive force of the pulse provides some electrons with the necessary momentum to cross the wakefield separatrix and be trapped in the wake. These electrons can then be accelerated to high energy. The same scheme is used in Ref. [10], but the authors show that wake-wake collisions, rather than the injection pulse ponderomotive force, can also give to some electrons the necessary momentum for injection and trapping. A third scheme [11] uses three laser pulses instead of two and operates in a collinear geometry. A pump pulse creates the wakefield while two other counterpropagating pulses collide inside the wake. Electrons are heated in the collision and, as in the first case, those with enough momentum are trapped. This scheme has then been simplified [8,12–14] by keeping the collinear geometry but only using two pulses. The pump pulse still creates the

wakefield but also collides with the second pulse, coming from the opposite direction. This collision, as previously, heats the electrons and some of them can then be trapped. Two counterpropagating laser pulses are also used in the cold optical injection scheme presented in this Letter. However, in this regime, injection relies on a fundamentally different mechanism as no momentum gain is needed. Here, during the collision with a very low-energy second pulse, the longitudinal electron motion is frozen and electrons can enter into the propagating wake, at a position allowing their injection. As a result of this mechanism, low-energy-spread electron bunches can be produced.

To introduce the cold injection principle, we present a 1D analysis which can give qualitative understanding of the physics involved. Electron motion in the wakefield is described by the Hamiltonian [12] $H(\psi, u_x) = [\gamma_\perp^2(\psi) + u_x^2]^{1/2} - \beta_p u_x - \Phi(\psi)$, where $\psi = x - \beta_p ct$ is the wake phase, $\beta_p = v_p/c$ with v_p the laser pulse group velocity and wake phase velocity, $\gamma_\perp = (1 + \mathbf{u}_\perp^2)^{1/2}$, $\mathbf{u}_\perp = \mathbf{p}_\perp/m_e c$ and $u_x = p_x/m_e c$ are the electron normalized transverse and longitudinal momenta, and $\Phi(\psi)$ is the wakefield potential. An electron at phase ψ_0 with a longitudinal momentum u_{x0} is characterized by $H_0 = H(\psi_0, u_{x0})$. The evolution of its longitudinal momentum is then

$$u_x(\psi) = \beta_p \gamma_p^2 [H_0 + \Phi(\psi)] \pm \gamma_p \sqrt{\gamma_p^2 [H_0 + \Phi(\psi)]^2 - \gamma_\perp^2(\psi)}, \quad (1)$$

where $\gamma_p = (1 - \beta_p^2)^{-1/2}$. The boundary between trapped and untrapped orbits (the separatrix) is given by a critical value, H_c , of the Hamiltonian. Its equation is thus

$$u_{xc}^{\pm}(\psi) = \beta_p \gamma_p^2 [H_c + \Phi(\psi)] \pm \gamma_p \sqrt{\gamma_p^2 [H_c + \Phi(\psi)]^2 - \gamma_{\perp}^2(\psi)}. \quad (2)$$

Figure 1 shows a typical separatrix and the fluid orbit of electrons in a wake favorable for cold injection. In this figure, the separatrix is well above the fluid trajectory indicating that self-injection cannot occur for electrons initially at rest. An interesting feature of Fig. 1 is the region where the separatrix is under the $u_x = 0$ axis. The existence of this large region indicates the possibility to inject electrons without giving them additional longitudinal momentum. If we can simply modify their motion so they can enter this region with negligible momentum, then they will be trapped. This is exactly what is done by the injection scheme proposed in this Letter.

To understand how a low-energy injection pulse can modify the electron motion and cause injection, we need to describe this electron motion during the collision of both pulses. Still, for the sake of simplicity, we present a 1D analytical description made with monochromatic laser waves and we consider the motion of an electron in vacuum. The normalized vector potentials of the two counter-propagating laser waves are, respectively, $\mathbf{A}_0 = (a_0/\sqrt{2})[\cos(\omega_0 t - k_0 x)\mathbf{e}_y + \sin(\omega_0 t - k_0 x)\mathbf{e}_z]$ and $\mathbf{A}_1 = (a_1/\sqrt{2})[\cos(\omega_0 t + k_0 x)\mathbf{e}_y + \sin(\omega_0 t + k_0 x)\mathbf{e}_z]$. The Hamiltonian of an electron in this field is $H(u_x, x) = \gamma = [1 + \mathbf{u}_{\perp}^2(x) + u_x^2]^{1/2}$, where $\mathbf{u}_{\perp} = \mathbf{A}_0 + \mathbf{A}_1$. The equation governing the evolution of the longitudinal momentum, u_x , is $d_t u_x = \partial H / \partial x = -(2\gamma)^{-1} d\mathbf{u}_{\perp}^2 / dx$, leading to

$$\frac{du_x}{dt} = \frac{1}{\gamma} k_0 a_0 a_1 \sin(2k_0 x). \quad (3)$$

This equation shows the existence of a beat wave force F , time independent and spatially oscillating with a $\lambda_0/2$ period. In comparison, the longitudinal ponderomotive force F_p , generated by the main pulse envelope, scales as $F_p \approx (2\gamma)^{-1} a_0^2 / (c\tau)$, where τ is the pulse duration. As $1/k_0 \ll c\tau$, we have $F/F_p \approx 2k_0 a_0 a_1 / (a_0^2 / c\tau) = 2\omega_0 \tau a_1 / a_0 > 1$. Thus, electrons are trapped inside the

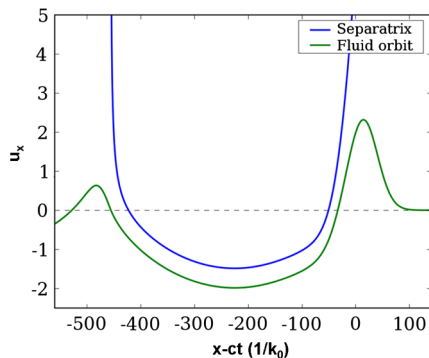


FIG. 1 (color online). Phase space plot of 1D fluid orbit and separatrix calculated in a typical case for cold optical injection.

$\lambda_0/2$ -long beat wave buckets and cannot have the large longitudinal motion normally caused by the ponderomotive force F_p .

To illustrate this mechanism, we consider two 30 fs, circularly polarized laser pulses with wavelength $\lambda_0 = 800$ nm. The pump pulse with energy of 4.2 J is focused to a $18 \mu\text{m}$ full width at half maximum (FWHM) focal spot. The peak normalized vector potential for this pulse is $a_0 = 4$. A 2 mJ injection pulse, propagating along the same axis but in the opposite direction, is focused to a $15 \mu\text{m}$ focal spot (FWHM) with a peak normalized vector potential $a_1 = 0.1$. The value of the plasma density is $n_e = 4.4 \times 10^{17} \text{ cm}^{-3} = 2.5 \times 10^{-4} n_c$, $n_c = m_e \epsilon_0 \omega_0^2 / e^2$ being the critical density and ϵ_0 the permittivity of free space. To model this setup, simulations have been run with the particle-in-cell code CALDER [15], in 2D geometry. The simulated on-axis wakefield has been used to plot Fig. 1.

Beat wave influence can be seen in Fig. 2(a) where the trajectory in the laboratory frame of an electron undergoing the collision and being injected (two pulse case) is compared to the trajectory of the same electron obtained in a simulation where the injection pulse is turned off (reference case). In this last case no electron is injected. The trajectory of the injected electron is representative of the other injected electrons. In the reference case, the electron is first pushed forward and sideways by the laser pondero-

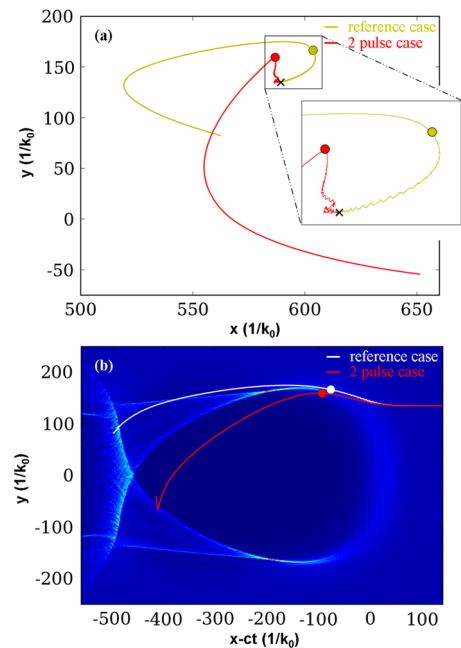


FIG. 2 (color online). Trajectories in laboratory frame (a) and wake frame (b) of an electron in simulations with injection pulse (two pulse case) or without (reference case). Both trajectories originate from the same point represented by a cross in (a). Dark gray (red) points and light gray (yellow) or white points represent electron position at $t = 820\omega_0^{-1}$, i.e., at the end of the collision in the two pulse case. The slow-evolving electron density map is plotted as background in (b).

motive force, and then its motion is determined by the wakefield. This electron is untrapped and slips backward in the wake frame. In comparison, the electron in the two pulse case is first trapped in a beat wave bucket. It is pushed sideways by the transverse ponderomotive force, but cannot move in the longitudinal direction on a distance greater than $\lambda_0/2$. As a consequence, just after the collision this electron is at a more backward position than in the reference case. Both electron trajectories are plotted in the wake frame in Fig. 2(b), together with the electron density computed in the reference simulation. Because of the collision, the wake generation is disturbed and inhibited [16]. However, as the pulse lengths are much shorter than the wake wavelength (approximately $10 \mu\text{m}$ compared to $60 \mu\text{m}$), the wakefield is not dramatically changed by the collision in our case. Using the reference electron density to analyze the trajectories in both cases is thus correct as a first approximation. Figure 2(b) indicates that after the collision, as the electron in the two pulse case is at a more backward position, it enters the blowout region. In this region, the wake transverse electric field is large and the electron is pulled towards the axis. Figure 3 represents the longitudinal momentum evolution with time for both electrons. For the two pulse case, in a first phase, the electron momentum oscillates slowly as it is trapped in the beat wave bucket. Then, the overlap of both laser pulses decreases and the beat wave force becomes weaker. Because of the fields of the back of the pump pulse, which still influences the electron, the electron momentum oscillates with a smaller period, as shown in Fig. 3. At the end of this collision phase, at time $t = 820\omega_0^{-1}$, the electron has gained a negligible longitudinal momentum. At this time, it is located inside the blowout region, as can be seen in Fig. 2(b) where its position is represented by a gray (red) point. Electron motion in the longitudinal direction is no longer restricted to the $\lambda_0/2$ beat wave bucket and the electron can move on a larger distance, as shown in

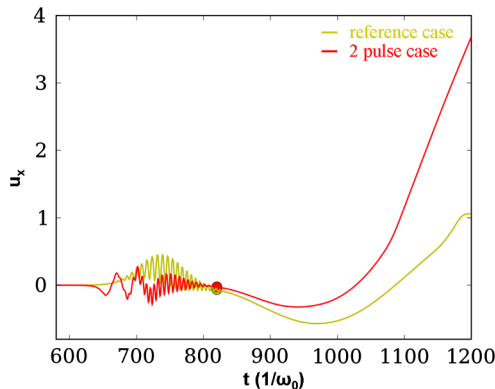


FIG. 3 (color online). Momentum evolution with time of an electron in simulations with injection pulse (two pulse case) or without (reference case). Dark gray (red) point and light gray (yellow) point represent electron momentum at time $t = 820\omega_0^{-1}$.

Fig. 2(a). Its position at this time is also represented by a dark gray (red) point in this figure. The electron can now be considered as injected, as it has been shifted backward in the wake by the collision, leading to its entry with negligible longitudinal momentum inside the region where $u_{xc}^- < 0$. It can then be accelerated to high energy.

Because of the laser and plasma parameters used in our simulation, the wake generation conditions are not far from the blowout regime [17] so multidimensional effects are important. Moreover, the electron is off axis when it enters the wake. However, as the longitudinal electric field in the blowout region is nearly constant in the transverse direction, the longitudinal momentum evolution of an on-axis or off-axis electron is not dramatically changed. 1D, on-axis analysis as it has been done then remains consistent, and can give the basic physical understanding of the process. This behavior is representative of the large majority of injected electrons, proving that injection relying on momentum gain due to the collision, as proposed in Refs. [11–13], is a different concept from the one discussed here.

This new injection mechanism can exist in our case because a higher pump pulse intensity than in Refs. [12,13] is used, leading to the generation of a large wake with a separatrix crossing the momentum axis $u_x = 0$ on a large region. Moreover, as previously described, operating at low plasma density allows us to use a wake wavelength much longer than pulse length, reducing wake inhibition during the collision. This is paramount for the injection of electrons, as they can therefore be accelerated by the regular wakefield just after the collision.

To underline the importance of this trajectory modification due to beat wave for injection, we have run an additional simulation where only the injection pulse polarization is changed. Circular polarization is still used but now rotates in the opposite direction. The normalized vector potential is then $\mathbf{A}_1 = (a_1/\sqrt{2})[-\cos(\omega_0 t + k_0 x)\mathbf{e}_y + \sin(\omega_0 t + k_0 x)\mathbf{e}_z]$. For infinite pulse, Eq. (3) becomes $d_t u_x = 0$, so no beat wave occurs for this polarization case. For real, finite duration pulses, the ponderomotive force of the injection pulse and its wake could disturb the main wake evolution, and can cause energy gain as in Refs. [9,10]. However, no injection is observed

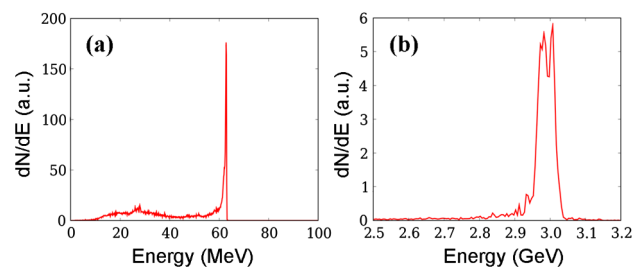


FIG. 4 (color online). Electron distributions obtained after acceleration over 0.6 mm (a) and over 3.8 cm in a plasma channel (b).

in our simulation with these polarizations. This result emphasizes the particular role of beat wave. With injection pulse energy kept constant, only the presence of the beat wave can lead to injection.

The electron beam injected by this cold injection method has a very good quality as can be seen in Fig. 4(a), which represents the electron distribution calculated after acceleration over 0.6 mm. A 62 MeV and 50 pC monoenergetic bunch is being accelerated by the wake. The rms energy spread of electrons with energy over 60 MeV is 0.7 MeV. Because of the absence of heating during injection, electrons are injected in a small volume of the phase space, allowing this low value of energy spread. This proves the interest of this method to inject electron bunches with narrow absolute energy spread. The bunch is still at the back of the wake bucket, indicating that its acceleration is just beginning and much higher energy can be reached.

One of the interests of this injection scheme is to offer a method to inject electrons in a wake created in a low density plasma, well under the self-injection threshold. Higher electron energies are then potentially reachable, but longer acceleration distances are needed. As we operate in low density plasmas, self-focusing is not large enough to guide the main pulse over long distances. We have then run a different simulation using a plasma channel profile. Plasma density n_e is now parabolic in the transverse direction: $n_e(r) = (1 + r^2/R^2)n_{e0}$, where r is the radial position, $n_{e0} = 2.5 \times 10^{-4}n_c$ is the unchanged plasma density on axis, and $R = 27 \mu\text{m}$ is a value chosen to provide good guiding of the pump pulse. In such a plasma channel, 2D simulation shows that the pump pulse can propagate over a few cm and keep a relatively stable spot size and intensity, pump depletion being the main limiting mechanism. The use of a plasma channel does not change the injection mechanisms described above, and a very similar distribution to the one plotted in Fig. 4(a) is obtained after 0.6 mm of propagation after collision. The simulation has been continued, and the dephasing length is nearly reached after 3.8 cm of propagation. Figure 4(b) shows the electron distribution found after this acceleration. The 50 pC electron bunch has now reached an energy of 3 GeV. The rms energy spread of electrons above 2.9 GeV is 0.9%. Because of the difference between 2D and 3D geometry, higher energy is expected in the 3D case. Beam loading is found to be the main cause for the absolute energy spread increase. We have run a second simulation with $a_1 = 0.07$ instead of $a_1 = 0.1$ used previously. In this case, the beam charge is 28 pC, showing the interesting possibility of tuning the beam charge by changing the injection pulse energy, and energy spread is reduced to 0.45%. We have checked that apart from the charge injected, injection is very similar in both cases. However, as the charges are different, the wakefield modification due to beam loading is also different and explains the variation of

the energy spread values. As a result, if beam loading is optimized (which is beyond the scope of this Letter), very narrow energy spreads are potentially reachable. For $a_1 = 0.07$, the normalized rms emittance is 2.6π mm mrad and the rms bunch duration is 4.8 fs.

To conclude, we have presented an optical injection mechanism based on electron spatial trajectory modification. Only mJ energy is needed for the injection pulse. The beat wave created during the laser pulse collision is responsible for the trajectory modification. This scheme is able to inject electron bunches with narrow absolute energy spreads in the wake. As this injection can be achieved in low density plasmas, multi-GeV energy gain can be obtained, with an energy spread ultimately limited by beam loading.

This work was carried out in the framework of the ANR project ANR-05-NT05-2-41699.

*xavier.davoine@cea.fr

- [1] T. Tajima and J.M. Dawson, Phys. Rev. Lett. **43**, 267 (1979).
- [2] S. Mangles *et al.*, Nature (London) **431**, 535 (2004).
- [3] C.G.R. Geddes, Cs. Toth, J. van Tilborg, E. Esarey, C.B. Schroeder, D. Bruhwiler, C. Nieter, J. Cary, and W.P. Leemans, Nature (London) **431**, 538 (2004).
- [4] J. Faure, Y. Glinec, A. Pukhov, S. Kiselev, S. Gordienko, E. Lefebvre, J.-P. Rousseau, F. Burgy, and V. Malka, Nature (London) **431**, 541 (2004).
- [5] W.P. Leemans, B. Nagler, A.J. Gonsalves, Cs. Toth, K. Nakamura, C.G.R. Geddes, E. Esarey, C.B. Schroeder, and S.M. Hooker, Nature Phys. **2**, 696 (2006).
- [6] Nasr A.M. Hafz *et al.*, Nat. Photon. **2**, 571 (2008).
- [7] A. Butler, D.J. Spence, and S.M. Hooker, Phys. Rev. Lett. **89**, 185003 (2002).
- [8] J. Faure, C. Rechatin, A. Norlin, A. Lifschitz, Y. Glinec, and V. Malka, Nature (London) **444**, 737 (2006).
- [9] D. Umstadter, J.K. Kim, and E. Dodd, Phys. Rev. Lett. **76**, 2073 (1996).
- [10] R.G. Hemker, K.-C. Tzeng, W.B. Mori, C.E. Clayton, and T. Katsouleas, Phys. Rev. E **57**, 5920 (1998).
- [11] E. Esarey, R.F. Hubbard, W.P. Leemans, A. Ting, and P. Sprangle, Phys. Rev. Lett. **79**, 2682 (1997).
- [12] G. Fubiani, E. Esarey, C.B. Schroeder, and W.P. Leemans, Phys. Rev. E **70**, 016402 (2004).
- [13] H. Kotaki, S. Masuda, M. Kando, J.K. Koga, and K. Nakajima, Phys. Plasmas **11**, 3296 (2004).
- [14] X. Davoine, E. Lefebvre, J. Faure, C. Rechatin, A. Lifschitz, and V. Malka, Phys. Plasmas **15**, 113102 (2008).
- [15] E. Lefebvre *et al.*, Nucl. Fusion **43**, 629 (2003).
- [16] C. Rechatin, J. Faure, A. Lifschitz, V. Malka, and E. Lefebvre, Phys. Plasmas **14**, 060702 (2007).
- [17] W. Lu, C. Huang, M. Zhou, M. Tzoufras, F.S. Tsung, W.B. Mori, and T. Katsouleas, J. Comput. Phys. **63**, 247 (1986).